X-RAY EMISSION FROM THE SOLAR CORONA

I. L. Beygman and L. A. Vaynshteyn

[Translated from Akademiya Nauk SSSR, Fizicheskiy Institut imeni
P. N. Lebedeva, Preprint #104, Moscow, 1967]
30 pages

Translated by
TECHTRAN CORP.
Glen Burnie, Md.
under Contract NAS 5-14826
#15

X-Ray Emission From The Solar Corona
I. L. Beygman and L. A. Vaynshteyn

1. Introduction

A number of new experimental data have recently become available on the spectrum of the solar corona in the X-ray region (1-30 Å) [1, 2]. In this paper the spectrum is theoretically calculated with a number of refinements as compared to the computations of previous authors [3, 4]. Specifically, dielectronic recombination and photorecombination on all levels were taken into consideration in calculating the ionization equilibrium. A computer was used for determining the effective cross sections of excitation, ionization, dielectronic recombination and photorecombination necessary for calculating population intensities.

2. Computation of Cross Sections and Rates of Elementary Processes

The X-ray spectrum is formed by emission of ions of high multiplicity. The effective excitation cross sections for the ions were calculated in the Born-Coulomb approximation in which the outer electron is described by the Coulomb wave function, as distinct from the ordinary Born approximation. The error in this method decreases with an increase in Z, and is no more than 20% for $Z \geqslant 5$. Here and in the following discussion, Z coincides with the spectroscopic symbol for the ion (e.g. $Z = 4$ for C^{IV}), i.e., the multiplicity of the ion is equal to $Z - 1$.

Calculation of ionization cross sections in the Born-Coulomb approximation is extremely cumbersome. However, the effect of the Coulomb field in this case is insignificant, and the Born approximation may be used [5]. When $\Delta E \lesssim 6k/T$, the error is no greater than 30%.

It is shown in Reference 6 that under the conditions in the corona, an appreciable part may be played by nonradiative ion capture of an electron to the self-ionization level (dielectronic recombination). The cross section of this process may be expressed in terms of the value of the excitation cross section of the ion at the threshold. The latter cross-section was also calculated in the Born-Coulomb approximation.

All cross sections were calculated on a computer according to a unified program. Single-electron semi-empirical atomic wave functions were used [7], the functions of the continuous spectrum (in calculating the cross sections of ionization and photorecombination) being found in the same field as those of the discrete state.

The resultant cross sections were used for calculating the rates of the elementary processes averaged with respect to the Maxwell energy distribution of the electrons $\langle v\sigma \rangle$.

In calculating σ and $\langle v\sigma \rangle$, it is convenient to use the dimensionless quantities

$$u = \frac{E - \Delta E}{\Delta E}; \qquad \beta = \frac{\Delta E}{kT} \tag{1}$$

as the argument in place of electron energy E and temperature T, where ΔE is the threshold energy of excitation or ionization. The relationship between $\langle v\sigma \rangle$ and β was approximated by an analytical formula with two parameters A and x, which were determined by the method of least squares with respect to the numerical values of $\langle v\sigma \rangle$. The calculation of $\langle v\sigma \rangle$ and determination of the parameters A and x were done on a computer within the framework of the same general program.

The following approximation formulas were used for describing the four elementary processes mentioned above.

Excitation to the state $n_0 l_0^q$:

$$\begin{aligned} \langle v\sigma_{01} \rangle &= C \left(\frac{\Delta E}{R_y}\right)^{1/2} e^{-\beta} \beta^{3/2} \int_0^\infty (1+u) \frac{\sigma_{01}(u)}{\pi a_0^2} e^{-\beta u} du \simeq \\ &\simeq 10^{-8} \left(\frac{E_1}{E_0} \frac{R_y}{\Delta E}\right)^{3/2} \cdot \frac{q}{2l_0+1} e^{-\beta} \frac{A\sqrt{\beta(\beta+1)}}{\beta+\chi} [\text{см}^3 \text{сек}^{-1}] \\ C &= \frac{2\sqrt{\pi}\, a_0 \hbar}{m} = 2{,}18 \cdot 10^{-8} [\text{см}^3 \text{сек}^{-1}] \end{aligned} \tag{2}$$

Here E_0 and E_1 are the energies of the lower and upper levels of the atom (reckoned from the ionization boundary); $R_y = \frac{e^2}{2a_0} = 13.6$ ev is the Rydberg unit equal to the ionization potential of hydrogen.

Ionization from the state $n_0 l_{0\infty}^q$:

$$\langle v\sigma_i\rangle = c\left(\frac{\Delta E}{R_y}\right)^{1/2} e^{-\beta}\beta^{3/2}\int_0^\infty (u+1)\frac{\sigma_i(u)}{\pi a_0^2}e^{-\beta u}du \simeq$$
$$\simeq 10^{-8}\left(\frac{R_y}{\Delta E}\right)^{3/2}\frac{q}{2l_0+1}e^{-\beta}\frac{A\sqrt{\beta}}{(\beta+\chi)\sqrt{\beta+1}}\ [\text{см}^3\text{сек}^{-1}] \tag{3}$$

Photorecombination

$$\langle v\sigma_r\rangle = c\left(\frac{\Delta E}{R_y}\right)^{1/2}\beta^{3/2}\sum_j\int_0^\infty u\,\frac{\sigma_r^{(j)}(u)}{\pi a_0^2}e^{-\beta u}du + R(\beta) \simeq$$
$$\simeq 10^{-16}\left(\frac{\Delta E}{R_y}\right)^{1/2}\cdot\frac{A\beta^{3/2}}{\beta+\chi}\ [\text{см}^3\text{сек}^{-1}] \tag{4}$$

where the summation is done with respect to a group of lower levels (in this paper with respect to levels with the principal quantum number of the ground state), and $R(\beta)$ is the contribution made by recombination to higher states. $R(\beta)$ was calculated by the Kramers formula (see Appendix 1). If $\Delta E \gg kT$ for the ground state, recombination is basically to the excited levels.

The case of dielectronic recombination requires further explanation. In computing the rate of dielectronic recombination χ_d, summation with respect to the aggregate of self-ionization levels $\gamma_1 nl$ is required instead of integration with respect to the continuous electron spectrum. If it is assumed that the exponential factor is identical for all levels, and integration is substituted for summation with respect to n, we get the simple analytical formula

$$\chi_d = 10^{-16}\alpha A\beta^{3/2}e^{-\beta};\qquad \beta = \frac{E_{01}^{(Z+1)}}{kT} \tag{5}$$

where $E_{01}^{(Z+1)}$ is the excitation energy for the resonance level of initial ion $B^{(Z+1)}$; for the two types of transitions of greatest interest in this ion, we have:

$\alpha = q/2l_0 + 1$ for the transition $l_0^q \rightarrow l_0^{q-1}l_1$

$\alpha = 2 - q/2l_1 + 1$ for the transition $l_0^N l_1^q \rightarrow l_0^{N-1}l_1^{q+1}$, $N = 2(2l_0 + 1)$.

A more detailed derivation of (5) and also an expression for A in terms of the excitation cross section of ion $B^{(Z+1)}$ are given in Appendix 2. Thus there is no need for using the method of least squares in the case of dielectronic recombination.

The factor which characterizes the order of magnitude of $\langle v\sigma \rangle$ is isolated in formulas (2)-(5). When determined in this way, the parameters A for different transitions in different ions vary over a comparatively narrow range. Parameters A and x for typical ions are given in Tables 1 and 2. These parameters are practically independent of Z for photorecombination, and nearly independent of Z and q for excitation and ionization. As may be seen from Table 2, A is somewhat more dependent on Z for dielectronic recombination.

The cross sections which we have used are appreciably different in some cases from those used in the literature [8, 9, 10]. These cross sections are usually calculated from empirical formulas which describe the different transitions in different ions "on the average". It is natural to suppose that the cross sections derived in this paper by numerical calculation for each state are more reliable. The maximum error resulting from approximate methods and wave functions is hardly greater than 30%. Because of this difference in cross sections, the ionization curves and temperature evaluations which we found without taking account of dielectronic recombination differ somewhat from those given in [1, 10] in some cases.

3. Ionization Equilibrium

Under conditions in the solar corona, the ratio between concentrations of two neighboring ions of a single element is determined by the ratio between the rates of recombination (radiative and dielectronic) and ionization:

$$\frac{N_Z}{N_{Z+1}} = \frac{\langle v\sigma \rangle + \mathcal{H}_d}{\langle v\sigma_i \rangle} \equiv P_Z \tag{6}$$

Hence for the relative concentration n_Z of ion Z, we have

$$n_Z = \frac{N_Z}{\sum_{Z'} N_{Z'}} = \frac{\prod_{j=1}^{Z} P_j}{\sum_{Z'} \prod_{j=1}^{Z'} P_j} \tag{7}$$

Under conditions in the solar corona, dielectronic recombination may be considerably attenuated by photoionization from high levels due to emission from the photosphere. However, it may be shown that photoionization has practically no effect in the case of helium-like ions, but is appreciable for ions with a large number of electrons.

TABLE 1

Parameters A and x for Cross Sections of Ionization and Excitation (All Transitions Without Change of Spin)

Element		A	χ
O VII	Ionization	9,2	0,65
	$1s^2 - 1s2p$	I8,6	0,22
	$1s^2 - 1s3p$	I6	0,28
Ca XVIII	Ionization	II,9	I,I
	$2s - 3p$	3,7	0,I6
	$2s - 4p$	2,4	0,I8
Fe XVII	Ionization*	29	0,98
	$2s^2 2p^6 \rightarrow 2s^2 2p^5 3d$	46	0,33
	$2s^2 2p^6 - 2s^2 2p^5 4d$	34	0,38
	$2s^2 2p^6 - 2s^2 2p^5 3s$	0,57	0,I5
	$2s^2 2p^6 - 2s^2 2p^5 4s$	0,49	0,I9

*Including ionization from the $2s^2$ shell

TABLE 2

Parameters A and x for Recombination Cross Sections of Oxygen and Calcium Ions (The Ion Resulting After Recombination is indicated in the Table)

Oxygen				Calcium			
Ion (Z)	Dielec. Recomb. $A.10^{-3}$	Dielec. Recomb. χ	Photo recomb. A.IO[illegible]	Ion (Z)	Dielec. Recomb. $A.10^{-3}$	Dielec. Recomb. χ	Photo Recomb. A.IO[illegible]
УШ	0,96	I,I	-	XX	0,96	I,I	-
УП	0,68	I,I	0,56	XIX	0,7I	I,2	0,II
УI	5,2	I,6	0,45	XУШ	5,8	I,7	0,I0
У	4,0	I,6	I5	XУП	5,4	I,7	I0
IУ	4,2	I,3	I4	XУI	5,5	I,8	I0
Ш	3,4	0,93	8,2	XУ	6,5	I,4	I0
П	2,2	0,36	5,I	XIУ	6,I	I,4	I0
I	0,83	0,05	I,65	XШ	4,8	I,4	9,5
				XП	3,7	I,7	8,9
				XI	3,3	I,8	8,4

It may be assumed in calculating the ionization rate that all ions are in the ground state. The fact that ionization is possible in some cases from the excited terms of the main configuration is inconsequential since the cross sections for ionization from an individual term and from a group of terms of a single configuration are identical*.

Shown in Figures 1 and 2 are the ionization curves for oxygen and calcium plotted with and without regard to dielectronic recombination. Table 3 gives the relative concentrations of ions for the most abundant elements in the solar corona, also found with and without regard to dielectronic recombination.

Only hydrogen-like and helium-like ions are well represented for all elements except iron and calcium. Dielectronic recombination is altogether impossible for hydrogen-like ions. In the case of helium-like ions, this type of recombination leads to a considerable increase in concentration in those cases where the ionization energy ΔE is less than kT, i.e., to the right of the maximum on the ionization equilibrium curve. The shift in the maximum in this case is insignificant. It should be noted that as Z increases, the rate of photorecombination increases in proportion to Z while the rate of ionization decreases in proportion to $1/Z^3$. Therefore the quantity E_Z/kT at the maximum of the ionization curve for ion Z decreases. As a result, the part played by dielectronic recombination increases with a rise in the multiplicity of the ion for helium-like ions.

---

*By definition, the ionization cross-section includes summation with respect to the moments of the final state.

(The set γ is the set of quantum numbers of the electron configuration).

$$\sigma_i(\gamma L S) = \sum_{L'S'} \sigma_i(\gamma L S \rightarrow \gamma' L' S') \tag{8}$$

If the distance between terms is considerably less than the energy of the level, this quantity is independent of LS. Therefore

$$\sigma_i(\gamma) = \frac{1}{g_\gamma} \sum_{LS} g_{LS}\, \sigma_i(\gamma L S) = \sigma_i(\gamma L S) \tag{9}$$

since the statistical weights obviously satisfy the condition

$$g_\gamma = \sum_{LS} g_{LS}$$

4. Radiation Flux in the Continuous Spectrum and in Lines

The flux close to the earth due to emission from the solar corona may be given in the form:

$$I = \frac{N_e^2 V}{4\pi R^2} J(\nu, \Delta\nu, T) \left[\frac{\text{erg}}{\text{Cm}^2 \text{Sec}}\right] \tag{10}$$

where N_e is electron density, V is the radiating volume of the corona, R is the distance from the Earth to the sun, the function N_e^2 I $(\nu, \Delta\nu, T)$ gives the total radiation flux from a unit volume of the solar corona in the frequency range from ν to $\nu + \Delta\nu$.

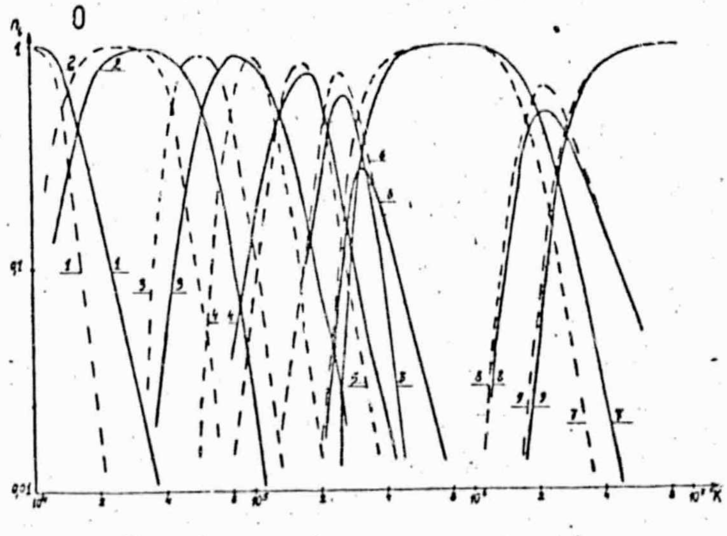

Figure 1. Relative Concentrations of Oxygen Ions as a Function of Temperature: Broken Curves -- Without Considering Dielectronic Recombination; Solid Curves -- Taking Dielectronic Recombination into Account.

The continuous spectrum is made up of bremsstrahlung and recombination radiation. It is sufficient in recombination radiation to consider transitions only to levels with the principal quantum number of the ground state. Using the Kramers approximation, we get

$$J_{\text{непр.}}(\lambda) = \frac{128\pi^{3/2} c\, a_0^3 R_y}{3\sqrt{3} \cdot 137^3} \sum_{a,z} \alpha^{(r)} n_z^{(a)} \left[z^2 \left(\frac{R_y}{\kappa T}\right)^{1/2} + \theta(\hbar\omega - \Delta E) \cdot 2 z \beta^{3/2} e^{\beta} \right] e^{-\frac{\hbar\omega}{\kappa T}} \frac{\Delta\lambda}{\lambda^2} \tag{11}$$

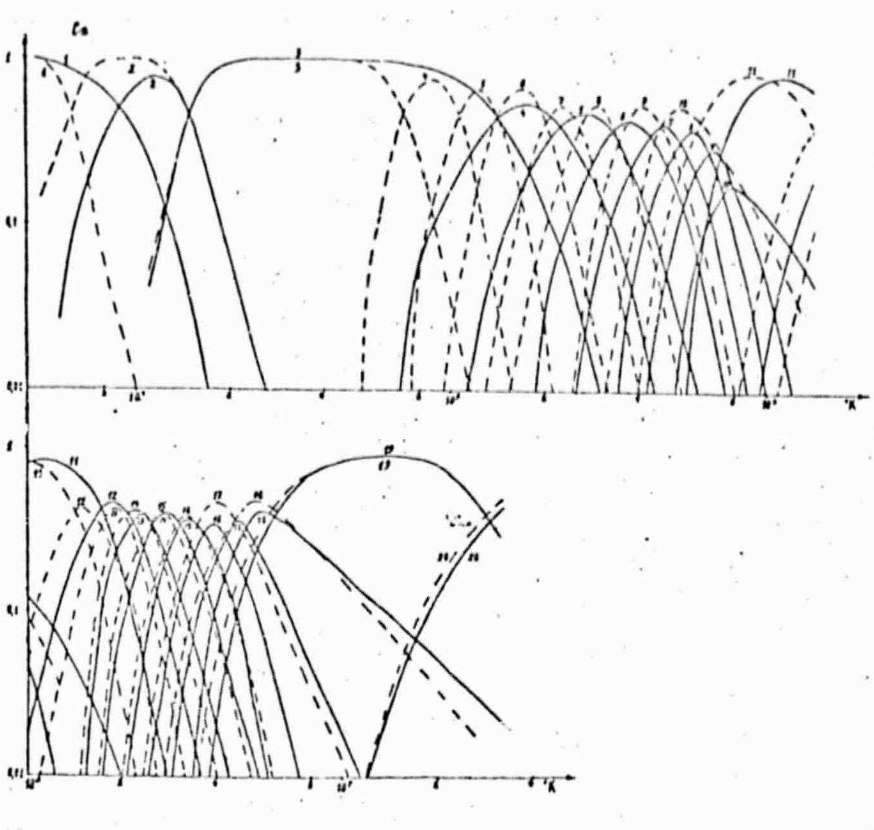

Figure 2. Relative Concentrations of Calcium Ions as a Function of Temperature: Broken Curves -- Without Considering Dielectronic Recombination; Solid Curves -- Taking Dielectronic Recombination into Account.

TABLE 3

Relative Concentrations n_Z and x-radiation Intensities I ($ergs/cm^2 sec$) in Lines of the Most Abundant Elements

Low Transition	α	λ A°	without dielec. recomb. 10^{6}°K		2.10^{6}°K		4.10^{6}°K		with dielec. recomb. 10^{6}°K		2.10^{6}°K		4.10^{6}°K		exp. (Ref. 1)
			n_z	J	n_z	J	n_z	J	n_z	J	n_z	J	n_z	J	
I	2	3	4		5		6		7		8		9		I0
N VI	-4 I5*/		0 85		-I 39		-3 30		0 87		0 I3		-2 24		
1s-2p		28,75		-2 22		-3 93		-4 2I		-2 22		-2 3I		-3 I7	
-3p		24,95		-3 26		-3 I6		-5 42		-3 26		-3 53		-4 34	
N VII			0 I5		0 46		-I 47		0 I2		0 4I		-I 47		
1s-2p		24,77		-3 I0		-2 44		-2 I5		-4 86		-2 40		-2 I6	-3 40
-3p		20,97		-5 90		-3 63		-3 29		-5 73		-3 57		-3 29	
O VII	-3 9I		0 99		0 38		-2 53		0 99		0 56		-I 29		
1s-2p		2I,56		-2 46		-I 37		-2 22		-2 45		-I 55		-I I2	-2 32
-3p		I8,57		-3 37		-2 5I		-3 39		-3 37		-2 76		-2 2I	-3 32
O VIII			-2 72		0 54		0 I8		-2 69		0 38		0 I7		
1s-2p		I8,87		-5 77		-I 20		-I 34		-5 73		-I I4		-I 33	-3 36
-3p		I6,08		-6 52		-2 25		-2 60		-6 50		-2 I8		-2 59	-4 59

*The characteristic and mantissa of the number are given, e.g. -415 means $0.15 \cdot 10^{-4}$

TABLE 3 (Cont'nued)

I	2	3	4	5	6	7	8	9	I0
Ne IX	-4 8I		0 88	0 94	0 2I	0 88	0 95	0 44	
1s-2p		I3,69	-5 78	-3 85	-2 2I	-5 57	-3 85	-2 42	
-3p		II,49	-7 32	-4 I3	-4 50	-7 32	-4 I3	-3 I0	
Ne X			-4 23	-I 4I	0 63	-4 23	-I 35	0 45	
1s-2p		II,98	- */	-4 I4	-2 32	-	-4 I2	-2 23	
-3p		I0,25	-	-5 I2	-3 47	-	-5 II	-3 34	
Na X	-5 20		0 67	0 97	0 7I	0 64	0 96	0 8I	
1s-2p		I0,98	-7 I2	-5 82	-3 I2	-7 II	-5 82	-3 I4	
-3p		9,43	-9 34	-6 67	-4 I7	-9 33	-6 69	-4 20	
N XI			-6 I0	-2 20	0 28	-7 98	-2 I9	0 I6	
1s-2p		9,99	-	-8 48	-4 I8	-	-8 46	-4 II	
-3p		8,38	-	-9 26	-5 I9	-	-9 24	-5 II	
Mg XI	-4 25		0 28	0 92	0 9I	0 20	0 92	0 94	
1s-2p		9,I6	-8 46	-4 27	-2 I0	-8 34	-4 27	-2 I0	
-3p		7,83	-	-5 I6	-3 I2	-	-5 I7	-3 I3	
Mg XII			-9 75	-3 I8	-I 76	-9 55	-3 I8	-I 46	
1s-2p		8,44	-	-8 I7	-4 38	-	-8 I6	-4 22	
-3p		7,II	-	-	-5 44	-	-	-5 25	

*The intensity of this line is less than 10^{-10}

I	2	3	4	5	6	7	8	9	I0
Al XII	-5 I6		-I 44	0 79	0 96	-I 20	0 78	0 95	
1s-2p		7,74	-	-6 35	-4 32	-	-6 34	-4 32	
-3p		6,62	-	-7 I8	-5 35	-	-7 I7	-5 35	
Al XIII			-	-4 I3	-I I8	-	-4 I3	-I I7	
1s-2p		7,09	-	-	-6 23	-	-	-6 2I	
-3p		5,99	-	-	-7 2I	-	-	-7 20	
Si XIII	-4 32		-2 32	0 54	0 93	-2 I2	0 50	0 92	
1s-2p		6,65	-	-5 I0	-3 29	-	-6 98	-3 29	
-3p		5,49	-	-7 I6	-4 I3	-	-7 I4	-4 I3	
Si XIV			-	-6 70	-2 38		-6 65	-2 36	
1s-2p		6,I9	-	-	-6 46	-	-	-6 44	
-3p		5,24	-	-	-7 4I	-	-	-7 40	
S XIV	-4 20		-4 I4	0 30	0 2I	-7 98	-I 46	0 20	
2s-4p		23,38	-9 I9	-4 68	-3 I8	-	-4 I0	-3 I7	
-5p		20,98	-	-4 24	-4 74	-	-5 36	-4 73	
S XV			-7 I8	-I 56	0 78	-9 I2	-2 86	0 76	
1s-2p		5,2	-	-8 39	-4 38	-	-9 60	-4 37	
-3p		4,I9	-	-	-5 I0	-	-	-5 I0	
S XVI			-	-9 32	-3 I3	-	-	-3 I2	
1s-2p		4,78	-	-	-8 I8	-	-	-8 I7	
-3p		3,99	-	-	-				

TABLE 3 (Continued)

I	2	3	4	5	6	7	8	9	I0
Ca XV	-5 I4		-7 40	-I 96	-I 66	-9 I0	-2 57	0 29	
2p-3s		26,I	-	-6 92	-5 22	-	-7 56	-5 94	
-4s		I9,I	-	-6 I5	-6 54	-	-8 88	-5 24	
-3d		24,4	-	-4 2I	-3 I2	-	-5 30	-3 54	
-4d		I8,7	-	-5 96	-4 36	-	-6 57	-3 I6	
Ca XVI				-2 66	0 I7		-3 II	0 26	
2p-3s		23,9*	-	-7 22	-5 22	-	-9 30	-5 32	
-4s		I7,5*	-	-8 27	-6 44	-	-	-6 68	
-3d		22,7*	-	-5 I2	-3 I2	-	-7 20	-3 20	
-4d		I7,2*	-	-6 I8	-4 30	-	-9 30	-4 45	
Ca XVII				-3 4I	0 42		-5 I5	0 I9	
2s-3p		20,I*	-	-7 20	-3 I0	-		-4 46	
-4p		I5,I*	-	-8 32	-4 28	-		-4 I3	
Ca XVIII				-5 47	0 28		-8 83	-I 72	
2s-3p		I9,07	-	-9 II	-4 34	-		-5 89	
-4p		I4,28	-		-5 56	-		-5 I4	
Ca XIX				-7 I3	-I 56			-I I5	
1s-2p		3,I9	-	-	-	-		-9 3I	
Ca XX					-8 62			-8 I6	
1s-2p		2,99	-	-	-	-		-	

*An error of ~ 0.5 Å is possible.

I	2	3	4	5	6	7	8	9	I0
Fe XVII	-5 37			0 I2	0 38		-2 2I	0 24	
2p-3s		I6,77	-	-5 44	-4 30	-	-7 24	-4 I9	-3 I7
-4s		I3,48	-	-6 26	-5 94	-	-8 47	-5 6I	
-3d		I5,26	-	-4 56	-2 I4	-	-6 99	-3 93	-3 I2
-4d		I2,I6	-	-5 69	-3 3I	-	-6 I2	-3 20	
Fe XVIII			-	-3 58	0 30	-	-5 69	-I 97	
2p-3s		I5,88	-	-8 82	-4 22	-	-	-5 70	
-4s		I2,02	-	-9 75	-5 40	-		-5 I2	
-3d		I4,33	-	-6 I7	-3 58		-8 I3	-3 I9	
-4d		II,48	-	-7 I8	-3 II		-9 I3	-4 34	

where $\beta = \Delta E/kT$; ΔE is the ionization energy (it was assumed that this energy was identical for levels with different 1); λ is the wavelength in cm; $\alpha^{(a)}$ is the abundance of element (a); and $n_Z^{(a)}$ is the relative concentration of ion Z of element (a). The function

$$\theta(\hbar\omega - \Delta E) = \begin{matrix} 1 \text{ when } \hbar\omega \geqslant \Delta E \\ 0 \text{ when } \hbar\omega < \Delta E \end{matrix}$$

In calculating the intensity of the lines, only the population of levels due to electron collision from the ground state was taken into account. It may be shown that population due to photorecombination does not play an appreciable part in most cases.

For the line corresponding to transition $K \rightarrow K^1$ in ion Z of element (a), we have

$$J(a, Z, K, K') = \alpha^{(a)} n_Z^{(a)} \langle v\sigma_{oK} \rangle \frac{A_{KK'}}{A_K} \hbar \omega_{KK'} \tag{12}$$

where A_{KK^1} is the probability of the optical transition $K \rightarrow K^1$; A_K is the total probability of radiation decay of level K: $A_K = \sum_{K^1} A_{KK^1}$.

The photospheric values for abundance of the elements [11] were used in this paper. Data have recently become available [12] to the effect that the abundance of a number of elements in the corona (particularly iron) is considerably greater than the photospheric values. The results given below confirm this conclusion. However, the presently available data are apparently still insufficient for reliably determining the abundance of elements in the corona. This is of little consequence for the intensity of the continuous spectrum since this intensity is almost entirely determined by ions of hydrogen, helium and oxygen atoms for which the data in Reference 12 are close to the photospheric values.

The absolute values of intensity were calculated for Baumbach's measure of emission $N_e^2V = 3.2 \cdot 10^{49}$ cm^{-3}.

Line intensities for three temperatures with and without regard to dielectronic recombination are given in Table 3. Experimental data from Reference 1 are also given in this same table.

Shown in Figure 3 are the continuous spectrum (for a resolution $\Delta\lambda = 0.1$ Å) and lines in the 3-30 Å region plotted with regard to dielectronic recombination.

Although the temperature of the corona is of the order of 10^{6}°K, the radiation for lines from all elements except oxygen and nitrogen comes from active regions with a considerably higher temperature. Therefore, the results are given for temperatures of $2 \cdot 10^{6}$ and $4 \cdot 10^{6}$°K. Given in Table 4 is the total flux

$$J_{\text{cont.}} + \sum_{\lambda - \Delta\lambda \leqslant \lambda_{\kappa\kappa'} \leqslant \lambda} J(a, z, \kappa, \kappa') \tag{13}$$

for a number of temperatures at $\Delta\lambda = 1$Å.

5. Discussion of the Results

The contribution to the continuous spectrum from various elements and mechanisms is illustrated by Figure 4. In the region $\lambda > 17$ Å, practically all the continuous spectrum is due to bremsstrahlung by H^{+} and He^{2+} ions.

In the region $\lambda < 17$ Å, approximately half the intensity is due to recombination of the O^{7+} ion. The discontinuity in intensity at 16.7 Å in Reference 2 is at the limit of sensitivity. In Reference work 1, the intensity of the continuous spectrum is too low in view of the extremely low value of $\Delta\lambda < 0.01$ Å.

The absolute intensity of line O^{VII} (2p) in Reference 1 corresponds to a temperature of 10^{6}°K. Naturally, excessive significance should not be attached to this figure; it is only an indication that the product $N_e^2 V$ does not differ too much from the assumed value.

As a rule, the lines of other ions are hotter, and their intensity is considerably dependent on the model of the corona. Therefore if no specific assumptions are made concerning the model, the intensity ratios give only the lower limit of the temperature of active regions responsible for emission of the hotter line. Besides, as has already been pointed out, a possible error in the assumed values of abundance must also be kept in mind.

The effect of temperature on the ratio $I(O^{VII}\ 2p)/I(O^{VIII}\ 2p)$ is illustrated in Figure 5. Shown in Table 5 are the temperatures which we found from the relative intensities of lines O^{VII} and O^{VIII} as given in [1, 2].

TABLE 4

Intensity of X-Radiation (ergs/cm^2sec) for A Resolution of

$\Delta\lambda = 1$ Å

$T, 10^6$ °K / λ Å	0,5		I		2		3		4	
35	-5	39*)	-4	8I	-3	33	-3	5I	-3	60
34	-5	32	-4	77	-3	33	-3	52	-3	62
33	-5	26	-4	7I	-3	33	-3	53	-3	64
32	-5	2I	-4	66	-3	33	-3	53	-3	66
3I	-5	I6	-4	60	-3	32	-3	54	-3	67
30	-5	I3	-4	55	-3	32	-3	55	-3	69
29	-4	24	-2	22	-2	34	-2	I2	-3	88
28	-6	69	-4	44	-3	3I	-3	56	-3	72
27	-6	49	-4	38	-3	30	-3	59	-3	79
26	-6	35	-4	34	-3	29	-3	57	-3	76
25	-5	I5	-3	37	-2	48	-2	35	-2	26
24	-6	I5	-4	25	-3	29	-3	6	-3	99
23	-6	I0	-4	25	-3	27	-3	58	-3	87
22	-5	75	-2	45	-I	55	-I	36	-I	I3
2I	-7	34	-4	23	-3	3I	-2	II	-2	I2
20	-7	I8	-4	I2	-3	22	-3	54	-3	85
I9	-6	22	-3	38	-I	2I	-I	47	-I	36
I8	-8	38	-5	63	-3	20	-3	54	-3	88
I7	-8	23	-4	II	-2	2I	-2	72	-2	68
I6	-9	80	-5	67	-3	28	-3	73	-2	I8
I5	-9	23	-5	38	-3	32	-3	99	-2	I6
I4	-I0	68	-5	76	-2	II	-2	40	-2	55
I3	-I0	I0	-6	95	-3	I8	-3	79	-2	I4
I2	-II	I4	-6	42	-3	I5	-2	I2	-2	35
II	-I2	I2	-6	I4	-4	9I	-3	63	-2	I4
I0	-I4	64	-7	35	-4	72	-3	69	-2	I9
9	-I5	I5	-8	54	-4	2I	-3	24	-3	65
8	-I7	I3	-9	60	-5	97	-3	I7	-3	59
7	-		-I0	24	-5	28	-3	II	-3	53
6	-		-I2	28	-6	25	-4	20	-3	I5
5	-		-I5	33	-7	I0	-5	23	-4	28
4	-		-		-I0	43	-7	7I	-5	23
3	-		-		-I5	57	-I0	50	-8	I2
2	-		-		-		-		-I5	60
I	-		-		-		-		-	

*The characteristic and mantissa of the number are given, e.g. -5 39 means $0.39 \cdot 10^{-5}$.

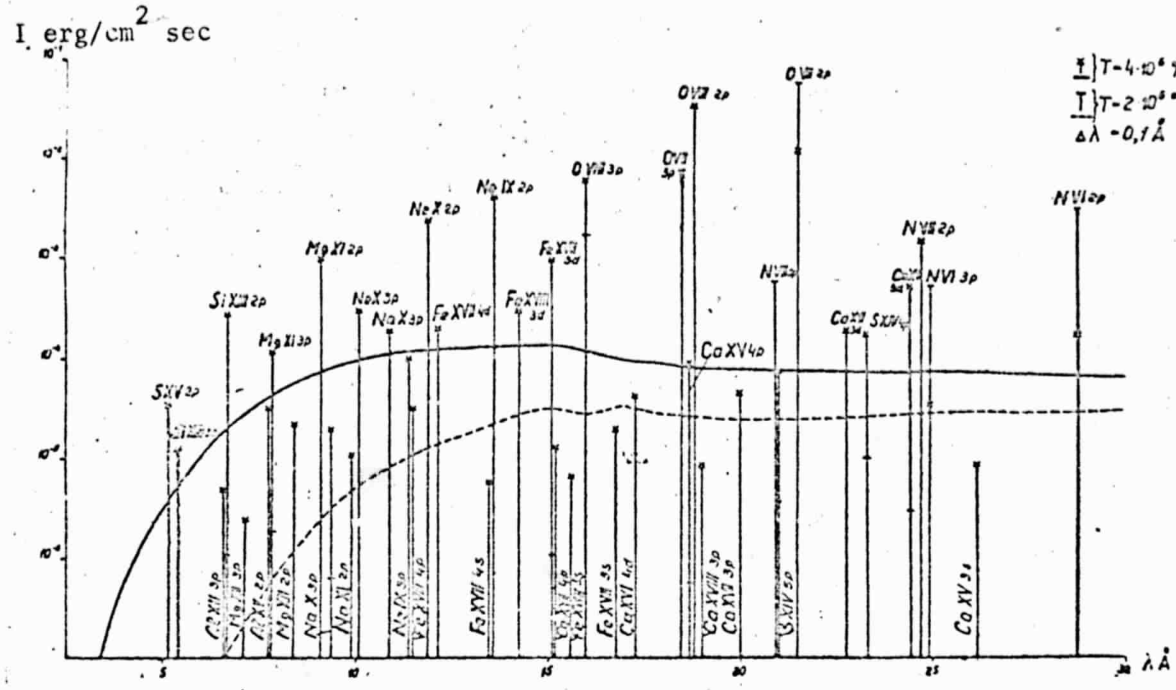

Figure 3. Spectrum of the Solar Corona Plotted with Regard to Dielectronic Recombination: Continuous Spectrum at a Resolution of $\Delta\lambda = 1$ Å -- Solid Curve for $T = 4 \cdot 10^6$ °K, Broken Curve for $T = 2 \cdot 10^6$ °K. Line Intensity is Designated by x for $T = 4 \cdot 10^6$ °K and by - for $T = 2 \cdot 10^6$ °K.

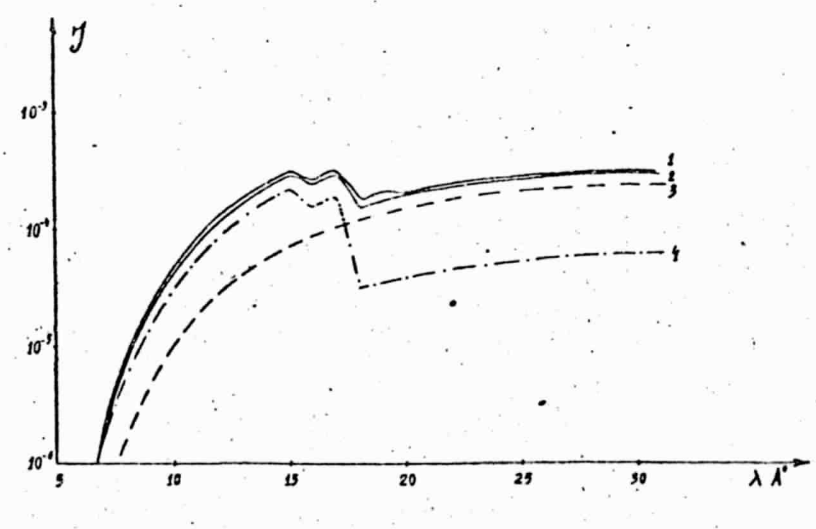

Figure 4. Continuous Spectrum at $T = 2 \cdot 10^6$ °K. 1--due to all elements; 2-4--due to hydorgen, helium and oxygen; 2--overall emission; 3--bremsstrahlung; 4--recombination radiation.

TABLE 5

	Intensity Ratio		Temp. T in 10^6 °K			
			with di. rec		without di. rec.	
	/1/	/2/	/1/	/2/	/1/	/2/
$O^{VII}\,2p / O^{VII}\,3p$	10	-	1,15	-	1,15	-
$O^{VII}\,2p / O^{VIII}\,2p$	9,1	-	1,6	-	1,7	-
$O^{VII}\,2p / (O^{VII}\,3p + O^{VIII}\,2p)$	4,8	2	1,5	1,9	1,6	2,3

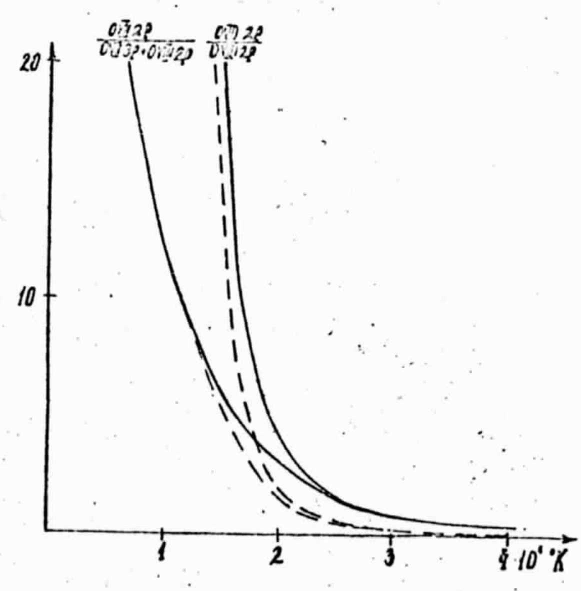

Figure 5. Intensity Ratio for Lines of Ions O^{VII} and O^{VIII} as a Function of Temperature: Broken curves -- Without Considering Dielectronic Recombination; Solid curves -- Taking Dielectronic Recombination into Account.

As might have been expected, the ratio O^{VII}/O^{VIII} gives a higher temperature since O^{VIII} shines chiefly from the active regions of the corona. The measurements in Reference 2 were made at a time of high coronal activity and therefore give a higher temperature (unfortunately, lines O^{VII} (3p) and O^{VIII} (2p) were not resolved in this work). We note that the given temperatures differ somewhat from those found in [1] due to the difference in cross sections (cf §2).

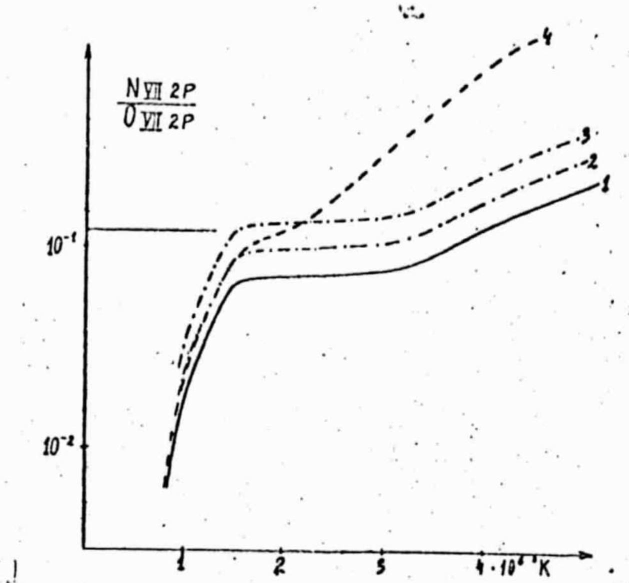

Figure 6. Intensity Ratio for the Lines of Ions N^{VII} and O^{VII} as a Function of Temperature: 1, 4--abundances According to Photospheric Data [11]; 2--Abundance According to Data of Ultraviolet Radiation [12]; 3--abundance According to Data of Solor Cosmic Rays [12]; 1-3--Calculations With Regard to Dielectronic Recombination; 4--Without Regard to Dielectronic Recombination; Horizontal line--Experimental Data of Reference 1.

Shown in Figure 6 is the effect of temperature on the ratio $I(N^{VII}$ 2p)/I (O^{VII} 2p) as well as experimental data from Reference 1 for comparison. Also shown in the figure are curves corresponding to oxygen and nitrogen abundances according to data of Reference 12 (ultraviolet emission from the corona and solar cosmic rays). These curves were plotted with regard to dielectronic recombination*.

*As noted in §3, the effect of photoionization on dielectronic recombination of helium-like ions is not appreciable.

Present computations support abundances according to solar cosmic rays. Calculations with the photospheric value of abundance are generally difficult to bring into agreement with experimental data.

The line intensity ratio $I(Fe^{XVII}\ 3d)/I(O^{VIII}\ 2p)$ given in Reference 1 is in even greater contradiction with the photospheric values of abundance. Calculations show that this ratio cannot be greater than 0.44, whereas the experiment gives a value of 3.6. Consequently the abundance ratio d(Fe)/d(0) is at least eight times the photospheric value. This problem is discussed in more detail in [13].

In conclusion, let us turn briefly to the transition $2p^6-2p^5 3s$ in the ion Fe^{XVII}. According to our calculations, the excitation cross section for the 3s level is lower than that of level 3d by approximately two orders of magnitude. At the same time, the experimental intensities of lines 2p-3s and 2p-3d are nearly identical. This is apparently due to successive population of the 3s state from terms $^{1,3}D$ and $^{1,3}F$ of 3d (transition 3d-3p-3s). Excitation of the latter terms is the result of electron collision chiefly due to exchange effects which were not considered in our calculations.

The authors are sincerely grateful to S. L. Mandel'shtam and I. A. Zhitnik for constructive criticism, and to A. V. Vinogradov for assistance with the calculations.

BIBLIOGRAPHY

1. Blake, R. L., T. A. Chubb, H. Friedman, A. E. Unzicker, Ap. J, 142, I, 1965.

2. Zhitnik, I. A., V. V. Krutov, L. P. Malyavkin, S. L. Mandel'shtam, and G. S. Cheremukhin, Kosmicheskiye issledovaniya, V. 274, 1967.

3. Fetisov, Ye. P., Kosmicheskiye issledovaniya, I, 209, 1963.

4. Elwert, G. Z., Naturforsch, 9a, 637, 1954.

5. Beygman, I. L., and L. A. Vaynshteyn, Astr. zh. (in press).

6. Burgess, A., Ap. J., 139, 776, 1964.

7. Vaynshteyn, L. A., Opt. i spektr. II, 301, 1961.

8. Seaton, M. J., Planet Space Sci., 12, 55, 1964.

9. Allen, C. W., Astrophysical Quantities, London, Athlone Press, 1963.

10. House, L., Ap. J., Supp., VIII, 307, 1964.

11. Goldberg, L., E. Müller, and L. Aller, Ap. J., Supp., 5, No. 45, 1960.

12. Pottasch, S. R., Ap. J. 137, 945, 1963.

13. Beigman, I., and L. Vainshtein, Astrophys. Lett. (in press).

Appendix 1

Rate of photorecombination

$$\langle V\sigma_r \rangle = \langle V\sigma_r^{(0)} \rangle + \sum_{j=1} \langle V\sigma_r^{(j)} \rangle + R(\beta)$$

Here $\sigma_r^{(0)}$ is the cross section of recombination to the ground state. For a configuration with equivalent electrons $n_0 l_0^q$ (in the ion after recombination), $\sigma_r^{(0)}$ differs from the case of a single electron by the factor

$$1 - \frac{q-1}{2(2l+1)}$$

The sum with respect to j includes several lower states. R(β) accounts for the contribution of all remaining levels. Using the Kramers approximation, we have

$$R(\beta) = \frac{32c}{3\sqrt{3}\ 137^3} \cdot Z \cdot \sum_{n=n_1}^{\infty} \beta_n^{1/2} E(\beta_n)$$

$$c = \frac{2\sqrt{\pi}\, a_0 h}{m}; \quad E(x) = -x e^{x} E_i(-x);$$

$$\beta_n = \frac{\Delta E_n}{KT} = \frac{Z^2 Ry}{KTn^2}$$

By substituting integration for summation with respect to n, it may be shown that

$$\beta_1 = \frac{\Delta E_1}{KT} = \frac{Z^2 Ry}{n_1^2 KT} = \beta \frac{\Delta E_1}{\Delta E_0}$$

Appendix 2

Let us examine the process of dielectronic recombination of the ion $B^{(Z+1)}$ in the ground state $\gamma 0$ through the intermediate self-ionization level $\gamma_1 nl$ of ion $B^{(Z)}$:

$$B^{(Z+1)}(\gamma_0)+e\rightarrow B^{(Z)}(\gamma_1 n\ell)\longrightarrow B^{(Z)}(\gamma_0 n\ell)+\hbar\omega \tag{1}$$

We shall assume that multiple ionization of ion $B^{Z}_{(\gamma_0 ne)}$ until it returns to the ground state is impossible. Both radiation transition with probability A and self-ionization with probability W are possible from level $\gamma_1 nl$. The balance equation takes the form:

$$N_{Z+1}N_e\, v\sigma_d(\gamma_1 n\ell)F(E)\delta E = N_{\gamma_1 n\ell}(W+A_{\gamma_1\gamma_0}) \tag{2}$$

where F(E) is the maximum electron energy distribution function, σ_d is the cross section for capture to the self-ionization level $\gamma_1 nl$, and δE is the width of this level. When A = 0, Saha distribution holds:

$$\left(\frac{N_{Z+1}N_e}{N_{\gamma_1 n\ell}}\right)_{\text{равн}} = S \equiv \frac{2g_{\gamma_0}}{g_{\gamma_1 n\ell}}\left(\frac{m\kappa T}{2\pi\hbar^2}\right)^{3/2} e^{\Delta E/\kappa T};$$

$$E_{10}=E_1^{(Z+1)}-E_0^{(Z+1)}; \qquad \Delta E = E_{10}-\frac{Z^2 R_y}{n^2}$$

where $Ry = e^2/2a_0$ is the Rydberg energy unit. It is assumed here and in the following discussion that n is large enough so that the $\gamma 0$ and $\gamma 1$ states of the inner electron may be treated as undisturbed states of ion $B^{(Z+1)}$. From (2) and (3), we find:

$$W = SFv\sigma_d\,\delta E = \frac{g_{\gamma_0}}{g_{\gamma_1 n\ell}}\,\frac{m^2v^2}{\pi^2\hbar^3}\,\sigma_d\,\delta E, \tag{4}$$

while the rate of recombination through level $\gamma 1$ is equal to

$$\mathcal{H}_d(\gamma_1)=\sum_{nl}\frac{N_{\gamma_1 nl}A_{\gamma_1\gamma_0}}{N_{Z+1}N_e}=\sum_{nl}\frac{1}{S}\frac{WA_{\gamma_1\gamma_0}}{W+A_{\gamma_1\gamma_0}}=$$

$$=A_{\gamma_1\gamma_0}\frac{g_{\gamma_1}}{g_{\gamma_0}}\left(\frac{2\pi\hbar^2}{m\kappa T}\right)^{3/2}\sum_{nl}(2l+1)e^{-\frac{\Delta E}{\kappa T}}\cdot\frac{1}{1+A_{\gamma_1\gamma_0}/W} \qquad (5)$$

The electron capture cross section $\sigma_d(\gamma_1 nl)$ may be expressed in terms of the partial cross section $\sigma_{\gamma_0\gamma_1}$ (l) for excitation of ion $B^{(Z+1)}$ for electron threshold energy $E = E_{10}$. Since $\sigma_{\gamma_0\gamma_1}$ at the threshold is independent of energy, it follows from considerations of continuity that:

$$\sum_{n=n'}^{n''}\sigma_d\,\delta E=\sigma_{\gamma_0\gamma_1}(l)(E''-E'),$$

if (n'' - n') corresponds to the same energy range in the region $E < E_{10}$ as $E'' - E'$ in the region $E > E_{10}$. Hence

$$\sigma_d\,\delta E=\sigma_{\gamma_0\gamma_1}(l)\frac{E''-E'}{n''-n'}=\frac{2Z^2R_y}{n^3}\sigma_{\gamma_0\gamma_1}(l) \qquad (6)$$

Using (6) and (4) and equalities $E = \Delta E$, $q_{\gamma_1 nl} = 2(2l + 1)q_{\gamma_1}$, we find

$$W=\frac{g_{\gamma_0}}{g_{\gamma_1}}\frac{(Z+1)^2\Delta E}{\pi\hbar n^3}\frac{\sigma_{\gamma_0\gamma_1}(l)}{\pi a_0^2(2l+1)} \qquad (7)$$

Finally, substituting (7) in (5) and replacing A by the oscillator strength f, we get

$$\mathcal{H}_d(\gamma_1)=\frac{4\pi^{3/2}\hbar}{m\,137^3}\left(\frac{E_{10}}{R_y}\right)^{1/2}f_{\gamma_0\gamma_1}\sum_{nl}(2l+1)\exp\left(\frac{Z^2R_y}{n^2\kappa T}\right)\frac{\beta^{3/2}e^{-\beta}}{1+an^3} \qquad (8)$$

$$a=\frac{\pi}{137^3}\left(\frac{E_{10}^2}{R_y\Delta E}\right)\cdot\frac{f_{\gamma_0\gamma_1}\pi a_0^2(2l+1)}{\sigma_{\gamma_0\gamma_1}(l)Z^2};\qquad \beta=\frac{E_{10}}{\kappa T} \qquad (9)$$

If the exponent is replaced by 1 in the sum with respect to n, assuming that $\Delta E \approx E_{10}$ and substituting integration for summation, we get a final expression for $\chi_d(\gamma 1)$ which, in accordance with formula (5) §2, may be expressed in the form

$$\varkappa_d = 10^{-16} \alpha A \beta^{3/2} e^{-\beta} \tag{10}$$

$$\alpha A = 540 \left(\frac{E_{10}}{R_y}\right)^{1/2} \tilde{f}_{01} \cdot \sum_{l} (2l+1)\, a^{-1/3} \Phi \tag{11}$$

$$\beta = \frac{\Delta E^{(z+1)}}{KT}; \qquad f_{01} = \alpha \tilde{f}_{01} \tag{12}$$

$$\Phi = a^{1/3} \int_{n_1}^{\infty} \frac{dn}{1+an^3} \simeq \frac{1}{2a^{2/3} n_1^2 + 0,8} \tag{13}$$

Here n_1 is the value of n for the lowest level (at the given l) where capture is still possible. Since ordinarily $a \ll 1$, the basic contribution to Φ is from levels with large n; f_{01} is the oscillator strength of the transition $n_0 l_0 - n_1 l_1$ in a single-electron atom.